BLIND IMAGE QUALITY ASSESSMENT FOR NOISE

Min Liu, Guangtao Zhai, Zhenyu Zhang, Yuntao Sun, Ke Gu, and Xiaokang Yang

Institute of Image Communication and Information Processing, Shanghai Jiao Tong University, Shanghai, China
Shanghai Key Laboratory of Digital Media Processing and Transmissions

ABSTRACT

Image denoising has been fanatically researched for a very long time in that it is a commonplace yet important subject. The task to testify the performance of different image denoising methods always resorts to PSNR in the past, until the emergence of SSIM, a landmark image quality assessment (IQA) metric. Since then, a vast majority of IQA methods were introduced in terms of various kinds of models. But unfortunately, those IQA metrics are along with more or less deficiencies such as the requirement of original images, making them far less than the ideal approaches. To address this problem, in this paper we propose an effective and blind image quality assessment for noise (dubbed BIQAN) to approximate the human visual perception to noise. The BIQAN is realized with three important portions, namely the free energy based brain principle, image gradient extraction, and texture masking. We conduct and compare the proposed BIQAN and a large amount of existing IQA metrics on three largest and most popular image quality databases (LIVE, TID2013, CSIQ). Results of experiments prove that the BIQAN has acquired very encouraging performance, outperforming those competitors stated above.

Index Terms— Image quality assessment (IQA), blind / no reference (NR), noise, free energy, image gradient, texture masking

1. INTRODUCTION

As noise being one of the most common distortions during the process of image acquisition, compression, transmission, and presentation, image denosing has become one of the most fundamental yet challenging problem in image processing and vision research. Naturally, how to judge image denosing becomes an intractable problem. Without doubt, the familiar topic of image quality assessment (IQA), which is an intensive research topic playing an important role in many areas of image processing, should be brought up for evaluating quality of noise-distorted images. Generally, IQA can be divided into subjective assessment and objective assessment. The objective assessment contained therein has been widely studied during the last decade, and it can also be fall into full-reference (FR) method, reduced-reference (RR) method, and no-reference (NR) method according to the availability of the reference image. In this paper, we concentrate on the NR IQA method for noise.

The studies of objective IQA metrics dated from decades ago. The traditional pixel-based indices, (e.g. mean-square error (MSE) and peak signal-to-noise ratio (PSNR)), are popular owing to their inexpensiveness and compatability. However, they are poorly correlated with human being's subjective rating, namely the mean opinion score (MOS) [1]. In 2004, the landmark structural similarity index (SSIM) which assumes that the human visual system (HVS) is highly concerned about the structural information was brought into the public by Wang *et al.* [2]. Besides, several sophisticated and state-of-the-art FR algorithms have been proposed during the last decade [3]-[14], e.g. the multi-scale SSIM (MS-SSIM) [3], the information fidelity criterion (IFC) [4], the visual information fidelity (VIF) [5], feature similarity index (FSIM) [9], gradient similarity index (GSM) [10], and internal generative model (IGM) [11]. RR IQA algorithms [15]-[19] have also attracted great interest of research. However, those FR and RR algorithms still require the whole or partial information of reference images.

Recently, a new NR metric scale invariant based noise estimator (SINE) [20] and its similar method [21] were proposed for noise-specific distorted images, which assume that the kurtosis values tend to be invariant across scales for a natural image and added noise will deteriorate this scale invariance. Nevertheless, these metrics are based on the condition that the distortion type is known. So several general purpose NR IQA metrics have be emphatically researched [22]-[29] in recent years. Besides, a noise level estimation algorithm [30] applies a PCA technique to estimate the noise level based on the weak texture patch dataset.

In this paper, a novel and robust blind image quality assessment for noise (BIQAN) is proposed to resort to the free-energy theory [31] induced structural model. The predicted image optimized by internal generative model from the distorted image can be used to simulate the original image [15]. So the IQA problem can be modeled as the estimation and comparison between the predicted and original images. Then the similarity map between these two images is realized based on a gradient modulus deduced similarity function, similar to [2]. Importantly, texture regions are believed to reduce the

visibility of noise, according to the principle of texture masking. Therefore a weighting function indicating the importance of texture region to HVS is utilized to pool the final quality score. In this paper, three databases including a wide range of noise images, LIVE [32], CSIQ [33] and the newly released image database TID2013 [34] are utilized as benchmarks in this paper.

The rest of this paper is arranged as follows. Section 2 puts forward our proposed BIQAN metric. Experimental results and comparative studies on the LIVE, CSIQ, and the newly proposed TID2013 databases are performed in Section 3. We conclude the whole paper in Section 4.

2. OUR PROPOSED BIQAN METRIC

Our proposed BIQAN index is composed of three stages. In the first stage, an free energy based internal generative model is used to obtain the predicted image from the distorted one. In the second stage, a similarity map is defined based on gradient map. In the last, the overall quality score is acquired by taking HVS based pooling map into consideration.

2.1. The review of free energy principle

According to our previous work [15], human cognitive process is governed by an internal generative model $\mathcal{G}$ in the brain, which is revealed by Friston in [31]. The generative model $\mathcal{G}$ adapts itself by by adjusting a parameter vector $\boldsymbol{\theta}$. We get the "surprise", which is defined by integrating the joint distribution over the space of model parameters $\boldsymbol{\theta}$, by observing the given image I

$$-\log\ P(I|\mathcal{G}) = -\log \int P(I,\boldsymbol{\theta}|\mathcal{G})d\boldsymbol{\theta} \tag{1}$$

By introducing an auxiliary term $Q(\boldsymbol{\theta}|I)$ into both the denominator and numerator into Eq. (1), we get

$$-\log\ P(I|\mathcal{G}) = -\log \int Q(\boldsymbol{\theta}|I)\frac{P(I,\boldsymbol{\theta}|\mathcal{G})}{Q(\boldsymbol{\theta}|I)}d\boldsymbol{\theta} \tag{2}$$

Then, by using Jensens inequality, we obtain the new equation

$$-\log\ P(I|\mathcal{G}) \leq -\int Q(\boldsymbol{\theta}|I)\frac{\log P(I,\boldsymbol{\theta})}{Q(\boldsymbol{\theta}|I)}d\boldsymbol{\theta} \tag{3}$$

The right hand of Eq. (3) is the definition of free energy

$$J(\boldsymbol{\theta}) = -\int Q(\boldsymbol{\theta}|I)\frac{\log P(I,\boldsymbol{\theta})}{Q(\boldsymbol{\theta}|I)}d\boldsymbol{\theta} \tag{4}$$

In this paper, we use a 2D linear autoregressive (AR) model to simulate the generative model $\mathcal{G}$ for its high recognition and description capability [35]. The AR model is defined as

$$x_i = \chi^k(x_i)\boldsymbol{\alpha} + e_i \tag{5}$$

where x_i is a pixel at location i, $\boldsymbol{\alpha} = (a_1, a_2, ...a_k)^T$ defines the model parameters, and $\chi^k(x_n)$ is the k member neighborhood vector of x_i. The model can be estimated by using the Bayesian information criterion (BIC) [36] as

$$\hat{\boldsymbol{\alpha}} = \arg\ \min_{\boldsymbol{\alpha}}(-\log\ P(I|\boldsymbol{\alpha}) + \frac{k}{2}\log\ N) \tag{6}$$

where N is the sample size. We should choose a fixed model order and training set size to simplify the method.

Given the k-th order piecewise AR model, we can write the linear equations as follows for a pixel x_i

$$x_i = \chi^k(x_i)\boldsymbol{\alpha} + e_i \qquad x_i \in \mathcal{N}(x_i) \tag{7}$$

where $\chi^k(x_i)$ is the model support and $\mathcal{N}(x_i)$ is the training set in a neighborhood of x_i. $\boldsymbol{\alpha}$ can be further written as follows

$$\hat{\boldsymbol{\alpha}} = \arg\ \min_{\boldsymbol{\alpha}} \parallel \mathbf{x} - \mathbf{X}\boldsymbol{\alpha} \parallel_2 \tag{8}$$

with $\mathrm{x} = (x_1, x_2, ..., x_N)^T$ and $\mathbf{X}(i,:) = \chi^k(x_i)$. The linear system can be solved easily as $\alpha = (\mathbf{X}^T\mathbf{X})^{-1}\mathbf{X}^T x$. The AR model is realized locally in a 7×7 neighborhood in our implementation.

2.2. BIQAN metric: gradient map based similarity

After acquiring the predicted image I_p from the distorted image I_d by the AR model, we calculate the similarity between images I_p and I_d. Gradient modulus (GM) is a commonly used feature which has been proved to be effective to noise-distorted images in our experiment. Many operators can be

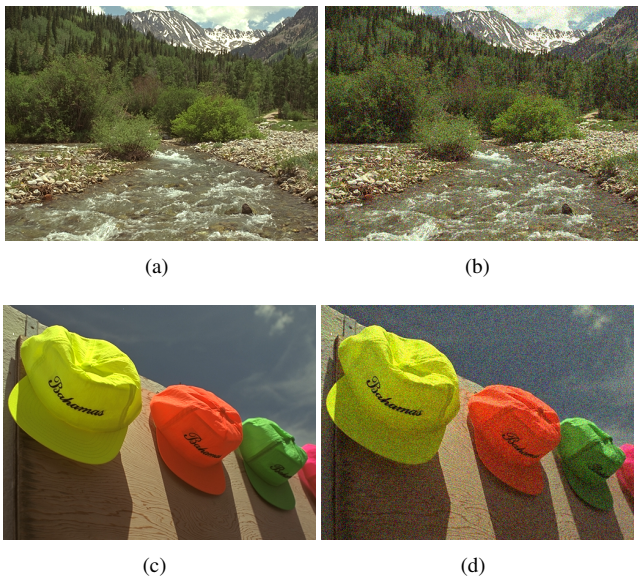

(a) (b) (c) (d)

Fig. 1: (a) and (c) are two original images from TID2013 database; (b) and (d) are two noise distorted images of (a) and (c) with the same distortion level.

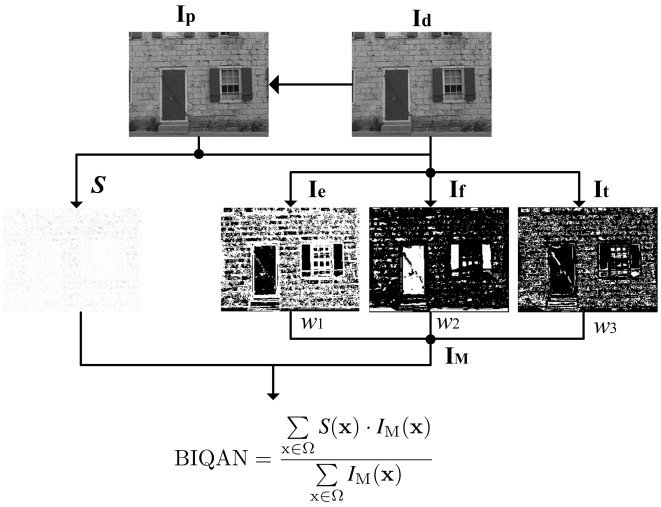

Fig. 2: Illustration of the computation of BIQAN metric.

adopted to compute the image gradient, e.g. the Sobel operator [37], the Prewitt operator [37], the Scharr operator [38], and we utilize the Scharr gradient operator in this paper. With Scharr gradient operator, partial derivatives $G_x(\mathbf{x})$ and $G_y(\mathbf{x})$ of an image are calculated as

$$G_x(\mathbf{x}) = \frac{1}{16}\begin{bmatrix} 3 & 0 & -3 \\ 10 & 0 & -10 \\ 3 & 0 & -3 \end{bmatrix} * \mathrm{I}(\mathbf{x}) \tag{9}$$

$$G_y(\mathbf{x}) = \frac{1}{16}\begin{bmatrix} 3 & 10 & 3 \\ 0 & 0 & 0 \\ -3 & -10 & -3 \end{bmatrix} * \mathrm{I}(\mathbf{x}) \tag{10}$$

The GM of $I(\mathbf{x})$ is then defined as $G(\mathbf{x}) = \sqrt{\mathrm{G_x^2}(\mathbf{x}) + \mathrm{G_y^2}(\mathbf{x})}$. GM maps extracted from images I_d and I_p are G_d and G_p separately. We define the similarity between the predicted and distorted images as

$$S(\mathbf{x}) = \frac{2G_d(\mathbf{x}) \cdot G_p(\mathbf{x}) + C}{G_d^2(\mathbf{x}) + G_p^2(\mathbf{x}) + C} \tag{11}$$

where C is a positive constant to avoid instability when $G_d^2(\mathbf{x}) + \mathrm{G}_p^2(\mathbf{x})$ is very close to zero, increasing the stability of $S(\mathbf{x})$.

Besides, as mentioned in [39], an image can be partitioned into three parts: edges, textures, and flat regions. More importantly, texture regions of images are less sensitive to noise distortion, in accordance with HVS. Just as images in Fig .1, the image (a) has more texture regions than image (c), while the noises in image (b) are less visible than those in image (d). Without doubt, different regions should have various weights to generate a good quality score pooling strategy correlating well with human visual fixation.

In this paper, we use a Scharr operator to segment images, and the templet is mentioned in the last subsection. We explore a similar solution to image participation.

1) Compute the gradient magnitudes by using a Scharr operation on the predicted (I_p) and distorted (I_d) images.

2) Determine thresholds $\mathrm{TH}_1 = \beta \times \mathrm{g_{max}}$ and $\mathrm{TH}_2 = \gamma \times \mathrm{g_{max}}$, where $g_{\max}$ is the maximum gradient magnitude value computed over the predicted image.

3) Assign pixels as belonging to smooth, edge and texture regions. We denote the gradient of pixel (i, j) on the predicted image is $g_p(i, j)$, and the gradient on the distorted image is $g_d(i, j)$, pixel classification is implemented based on the following rules:

(a) If $g_p(x, y) > \mathrm{TH}_1$ or $g_d(x, y) > \mathrm{TH}_1$, the pixel is considered as an edge pixel.

(b) If $g_p(x, y) < \mathrm{TH}_2$ and $g_d(x, y) \leq \mathrm{TH}_1$, the pixel belongs to a smooth region.

(c) Otherwise, the pixel is regarded as part of a textured region.

The edge region, smooth region and texture region of the image are I_e, I_s and I_t respectively. So the pooling map is calculated as

$$I_{\mathrm{M}} = w_1 \cdot I_e + w_2 \cdot I_s + w_3 \cdot I_t \tag{12}$$

where w_1 - w_3 are three weights for three different regions, and $w_1 + w_2 + w_3 = 1$. After obtaining the local similarity at each location , the overall similarity can be obtained. The BIQAN index to evaluate the overall image quality between I_p and I_d is defined as

$$\mathrm{BIQAN} = \frac{\sum\limits_{\mathrm{x}\in\Omega} S(\mathbf{x}) \cdot I_{\mathrm{M}}(\mathbf{x})}{\sum\limits_{\mathrm{x}\in\Omega} I_{\mathrm{M}}(\mathbf{x})} \tag{13}$$

where Ω indicates the whole image.

3. EXPERIMENTAL RESULTS AND DISCUSSIONS

Three databases containing noise distorted images, LIVE, CSIQ, and the newly proposed TID2013 are adopted as testing beds in our experiment. To illustrate, the details of these databases are tabulated in Table. 1. The quality assessment metrics used for comparison include FR metrics (PSNR, SSIM, MS-SSIM), NR algorithms (SINE, [30], DIIVINE, BLIINDS-II, BRISQUE, NIQE, QAC), and our proposed BIQAN.

Table 1: The details of three benchmark databases.

Dataset	Reference Images No.	Distorted Image. No	Distortion Types No.	Objects No.
LIVE	29	779	5	145
CSIQ	30	866	6	150
TID2013	25	3000	24	125

Table 2: PLCC, SROCC, KROCC and RMSE values (after nonlinear regression) of FR metrics (PSNR, SSIM, MS-SSIM) and NN metrics (SINE, [30], DIIVINE, BLIINDS-II, BRISQUE, NIQE, QAC) and our proposed BIQAN on noise distorted images from LIVE, CSIQ and TID2013 databases. We bold the best performance for specific evaluation.

		PSNR	SSIM	MS-SSIM	SINE	[30]	DIIVINE	BLIINDS-II	BRISQUE	NIQE	QAC	BIQAN
LIVE	PLCC	0.9868	0.9800	0.9821	0.8762	**0.9923**	0.9911	0.9685	0.9909	0.9729	0.9512	0.9919
	SROCC	0.9854	0.9629	0.9745	0.9837	0.9864	0.9878	0.9496	0.9911	0.9718	0.9509	**0.9880**
	KROCC	0.8939	0.8364	0.8653	0.8874	0.8989	**0.9098**	0.8006	0.9241	0.8538	0.7893	0.9052
	RMSE	1.5885	0.0648	0.0488	18.4082	3.1260	2.9501	6.9906	3.7911	4.3311	0.0761	**0.0074**
CSIQ	PLCC	0.9557	0.8967	0.8359	0.9518	0.9438	0.8757	0.7459	0.9239	0.7664	0.8489	**0.9593**
	SROCC	0.9363	0.9255	0.9088	0.9542	0.9471	0.8663	0.7597	0.9252	0.8098	0.8222	**0.9574**
	KROCC	0.7643	0.7543	0.7341	0.8072	0.7896	0.6774	0.5605	0.7538	0.6063	0.5938	**0.8181**
	RMSE	1.8690	0.0861	0.0169	1.6287	1.7162	7.3355	9.1733	6.0201	1.6350	0.0224	**0.0072**
TID 2013	PLCC	**0.9483**	0.8423	0.8213	0.8344	0.9471	0.8391	0.6528	0.8399	0.7575	0.8077	0.9281
	SROCC	0.9225	0.8528	0.8658	0.8381	0.9241	0.8510	0.6465	0.8492	0.8144	0.7414	**0.9244**
	KROCC	0.7535	0.6439	0.6626	0.6665	0.7525	0.6476	0.4536	0.6546	0.6048	0.5196	**0.7546**
	RMSE	1.3417	0.0843	0.0236	2.3609	0.6320	7.0465	7.8598	7.1474	2.1523	0.0547	**0.0082**
Database size -weighted average	PLCC	**0.9642**	0.9093	0.8820	0.8908	0.9615	0.9046	0.7950	0.9220	0.3842	0.8720	0.9613
	SROCC	0.9492	0.9168	0.9187	0.9298	0.9538	0.9037	0.7916	0.9254	0.3823	0.8426	**0.9581**
	KROCC	0.8058	0.7498	0.7581	0.7930	0.8163	0.7488	0.6115	0.7831	0.3313	0.6392	**0.8293**
	RMSE	1.6152	0.0782	0.0299	7.6395	1.8802	5.7355	8.0288	5.5861	2.7198	0.0505	**0.0076**

A four parameter logistic function was adopted to map the scores to subjective ratings:

$$q(\varepsilon) = \frac{\xi_1 - \xi_2}{1 + \exp(-\frac{\varepsilon - \xi_3}{\xi_4})} + \xi_2 \tag{14}$$

where ε is the input score, while $q(\varepsilon)$ is the mapped score, and ξ_1 to ξ_4 are free parameters to be determined during the curve fitting process. Four commonly used performance measures, Pearson's linear correlation coefficient (PLCC), Spearman's rank ordered correlation (SROCC), Kendall's rank-order correlation coefficient (KROCC), and Root mean-squared error (RMSE), which all suggested by VQEG [40] are utilized in this paper to evaluate and compare these IQA metrics.

The prediction performance of all metrics are tabulated in Table 2. It can be easily seen that our metric has better performance than all the other competing methods evaluated on CSIQ database no matter what performance criterion is used. It also achieves the best overall results than others on LIVE and TID2013 databases, which is higher SROCC and lower RMSE on LIVE database, higher SROCC KROCC and lower RMSE on TID2013 database.

4. CONCLUSION

In this paper, we propose a novel, efficient and robust IQA metric, namely BIQAN, based on the free energy principle, image gradient extraction and texture masking. Predicted images are reconstructed from the distorted ones based on free energy principle. Then a image gradient map induced similarity metric and edge, texture and flat segmentation according to their different cover degrees of noise are combined to form the final quality metric. Experimental results indicate that our algorithm outperforms many state-of-the-art metrics on noise distorted images from three benchmark databases LIVE, CSIQ and TID2013.

Acknowledgment

This work was supported in part by NSFC (61025005, 61371146, 61221001), 973 Program (2010CB731401) and FANEDD (201339).

5. REFERENCES

[1] Z. Wang and A. C. Bovik, "Mean squared error: Love it or leave it?-A new look at signal fidelity measures," *IEEE Signal Process. Mag.*, vol. 26, no. 1, pp. 98-117, January 2009.

[2] Z. Wang, A. C. Bovik, H. R. Sheikh, and E. P. Simoncelli, "Image quality assessment: From error visibility to structural similarity," *IEEE Trans. Image Process.*, vol. 13, no. 4, pp. 600-612, April 2004.

[3] Z. Wang, E. P. Simoncelli, and A. C. Bovik, "Multi-scale structural similarity for image quality assessment," *Proc. IEEE Asilomar Conf. Signals, Syst., Comput.*, pp. 1398-1402, November 2003.

[4] H. R. Sheikh, A. C. Bovik, and G. Veciana, "An information fidelity criterion for image quality assessment using natural scene statistics," *IEEE Trans. Image Process.*, vol. 14, 2005.

[5] H. R. Sheikh and A. C. Bovik, "Image information and visual quality," *IEEE Trans. Image Process.*, vol. 15, no. 2, pp. 430-444, 2006.

[6] G. Zhai, W. Zhang, X. Yang, S. Yao, and Y. Xu, "GES: a new image quality assessment metric based on energy features in Gabor transform domain," *Proc. IEEE Int. Symp. Circuits and Syst.*, pp. 1715-1718, 2006.

[7] G. Zhai, W. Zhang, Y. Xu, and W. Lin, "LGPS: Phase based image quality assessment metric," *IEEE Workshop on Signal Processing Systems*, pp. 605-609, 2007.

[8] G. Zhai, Q. Chen, X. Yang, and W. Zhang, "Scalable visual sensitivity profile estimation," *Proc. IEEE Int. Conf. on Acoustics, Speech and Signal Process.*, pp. 873-876, 2008.

[9] L. Zhang, L. Zhang, X. Mou, and D. Zhang, "FSIM: A feature similarity index for image quality assessment," *IEEE Trans. Image Process.*, vol. 20, no. 8, pp. 2378-2386, August 2011.

[10] A. Liu, W. Lin, and M. Narwaria, "Image quality assessment based on gradient similarity," *IEEE Trans. Image Process.*, vol. 21, no. 4, pp. 1500-1512, April 2012.

[11] J. Wu, W. Lin, G. Shi, and A. Liu, "Perceptual quality metric with internal generative mechanism," *IEEE Trans. Image Process.*, vol. 22, no. 1, pp. 43-54, January 2013.

[12] K. Gu, G. Zhai, X. Yang, L. Chen, and W. Zhang, "Nonlinear additive model based saliency map weighting strategy for image quality assessment," *IEEE International Workshop on Multimedia Signal Processing*, pp. 313-318, September 2012.

[13] K. Gu, G. Zhai, X. Yang, and W. Zhang, "A new psychovisual paradigm for image quality assessment: From differentiating distortion types to discriminating quality conditions," *Signal, Image and Video Processing*, vol. 7, no. 3, pp. 423-436, May 2013.

[14] M. Liu, G. Zhai, K. Gu, Q. Xu, X. Yang, X. Sun, W. Chen, and Y. Zuo, "A new image quality metric based on MIx-Scale transform," *Proc. IEEE Workshop on Signal Processing Systems*, pp. 266-271, October 2013.

[15] G. Zhai, X. Wu, X. Yang, W. Lin and W. Zhang, "A psychovisual quality metric in free-energy principle," *IEEE Trans. Image Process.*, vol. 21, no. 1, pp. 41-52, January 2012.

[16] R. Soundararajan and A. C. Bovik, "RRED indices: Reduced-reference entropic difference for image quality assessment," *IEEE Trans. Image Process.*, vol. 21, no. 2, pp. 517-526, February 2012.

[17] M. Narwaria, W. Lin, I. V. McLoughlin, S. Emmanuel, and L. T. Chia, "Fourier transform-based scalable image quality measure," *IEEE Trans. Image Process.*, vol. 21, no. 8, pp. 3364-3377, 2012.

[18] K. Gu, G. Zhai, X. Yang and W. Zhang, "A new reduced-reference image quality assessment using structural degradation model," *IEEE Int. Symp. Circuits and Syst.*, pp. 1095-1098, May 2013.

[19] K. Gu, G. Zhai, X. Yang, W. Zhang, and M. Liu, "Subjective and objective quality assessment for images with contrast change," *Proc. IEEE Int. Conf. Image Process.*, pp. 383-387, September 2013.

[20] D. Zoran and Y. Weiss, "Scale invariance and noise in natural images," *IEEE Int. Conf. Comput. Vis.*, pp. 2209-2216, 2009.

[21] G. Zhai, and X. Wu, "Noise estimation using statistics of natural images,"*IEEE Int. Conf. Image Process.*, pp. 1857-1860, September 2011.

[22] A. K. Moorthy and A. C. Bovik, "Blind image quality assessment: From scene statistics to perceptual quality," *IEEE Trans. Image Process.*, vol. 20, no. 12, pp. 3350-3364, December 2011.

[23] M. A. Saad, A. C. Bovik, and C. Charrier, "Blind image quality assessment: A natural scene statistics approach in the DCT domain," *IEEE Trans. Image Process.*, vol. 21, no. 8, pp. 3339-3352, 2012.

[24] A. Mittal, A. K. Moorthy and A. C. Bovik, "No-reference image quality assessment in the spatial domain," *IEEE Trans. Image Process.*, vol. 21, no. 12, pp. 4695-4708, December 2012.

[25] A. Mittal, R. Soundararajan, and A. C. Bovik, "Making a completely blind image quality analyzer," *IEEE Signal Processing Letters*, vol. 22, no. 3, pp. 209-212, March 2013.

[26] K. Gu, G. Zhai, X. Yang, and W. Zhang, "No-reference stereoscopic IQA approach: From nonlinear effect to parallax compensation," *Journal of Electrical and Computer Engineering*, vol. 2012, Article ID 436031, 2012.

[27] K. Gu, G. Zhai, X. Yang, W. Zhang, and L. Liang, "No-reference image quality assessment metric by combining free energy theory and structural degradation model," *Proc. IEEE Int. Conf. Multimedia and Expo*, pp. 1-6, July 2013.

[28] W. Xue, L. Zhang, and X. Mou, "Learning without human scores for blind image quality assessment," *IEEE Int. Conf. Computer Vision and Patter Recognition*, July 2013.

[29] K. Gu, G. Zhai, M. Liu, X. Yang, and W. Zhang, "Details preservation inspired blind quality metric of tone mapping methods," *Proc. IEEE Int. Symp. Circuits and Syst.*, June 2014.

[30] X. Liu, M. Tanaka, and M. Okutomi, "Noise level estimation using weak textured patches of a single noisy image," *IEEE Int. Conf. Image Process.*, pp. 665-668, 2012.

[31] K. Friston, "The free-energy principle: A unified brain theory?" *Nature Reviews Neuroscience*, vol. 11, pp. 127-138, 2010.

[32] H. R. Sheikh, Z. Wang, L. Cormack, and A. C. Bovik, "LIVE image quality assessment Database Release 2," [Online]. Available: http://live.ece.utexas.edu/research/quality

[33] E. C. Larson and D. M. Chandler, "Categorical image quality (C-SIQ) database," [Online]. Available: http://vision.okstate.edu/csiq

[34] N. Ponomarenko, O. Ieremeiev, V. Lukin, K. Egiazarian, L. Jin, J. Astola, B. Vozel, K. Chehdi, M. Carli, and F. Battisti, "Color image database TID2013: Peculiarities and preliminary results," in 4th European Workshop on Visual Information Processing, 2013.

[35] X. Wu, G. Zhai, X. Yang, and W. Zhang, "Adaptive sequential prediction of multidimensional signals with applications to lossless image coding," *IEEE Trans. on Image Processing*, vol. 20, no. 1, pp. 36-42, 2011.

[36] G. Schwarz, "Estimating the dimension of a model," *Annals of Statistics*, vol. 6, pp. 461-464, 1978.

[37] R. Jain, R. Kasturi, and B. G. Schunck , "Machine Vision". New York: McGraw-Hill, 1995.

[38] B. Jähne, H. Haubecker, and P. Geibler,"Handbook of Computer Visionand Applications". New York: Academic, 1999.

[39] J. Li, G. Chen, and Z. Chi, "Image Coding Quality Assessment Using Fuzzy Integrals With a Three-Component Image Model,"*IEEE Trans. on fuzzy system*, vol. 12, no. 1, February 2004.

[40] VQEG, "Final report from the video quality experts group on the validation of objective models of video quality assessment," March 2000, http://www.vqeg.org/